

Magnetic-Field Asymmetry of Nonlinear Transport in Carbon Nanotubes

Jiang Wei, Michael Shimogawa, Zenghui Wang, Iuliana Radu, Robert Dormaier, and David Henry Cobden*

Department of Physics, University of Washington, Seattle, Washington 98195-1560, USA

(Received 25 June 2005; published 12 December 2005; corrected 13 December 2005)

We demonstrate that nonlinear electrical transport through a two-terminal nanoscale sample is not symmetric in the magnetic field B . More specifically, we have measured the lowest order B -asymmetric terms in single-walled carbon nanotubes. Theoretically, these terms can be used to infer both the strength of electron-electron interactions and the handedness of the nanotube. Consistent with theory, we find that at high temperatures the B -linear term is small and has a constant sign independent of Fermi energy, while at low temperatures it develops mesoscopic fluctuations. We also find surprising magnetoresistance at zero bias in the metallic regime.

DOI: [10.1103/PhysRevLett.95.256601](https://doi.org/10.1103/PhysRevLett.95.256601)

PACS numbers: 72.20.Ht, 72.20.My, 73.63.Fg

The conductance G of a two-terminal sample in linear response must be an even function of applied magnetic field \mathbf{B} , that is, $G(\mathbf{B}) = G(-\mathbf{B})$ [1,2]. The underlying principle that leads to this Onsager symmetry is the time-reversal symmetry of fluctuations in equilibrium, combined with the fact that \mathbf{B} changes sign on time reversal. There is no such strong symmetry requirement for nonlinear response, which probes nonequilibrium effects. Nevertheless, some useful observations may also be made about the nonlinear transport coefficients defined by expanding the current I in powers of the voltage V :

$$I = G(B)V + \chi(B)V^2 + \dots, \quad (1)$$

and expanding the first nonlinear coefficient χ in powers of B :

$$\chi(B) = \chi_0 + \alpha B + \dots. \quad (2)$$

One observation is that, for a sample with helical symmetry, the sign of the coefficient α in Eq. (2) depends on the handedness [3,4]. This is essentially because the axial vector \mathbf{B} combined with the helicity defines a direction which is inverted if \mathbf{B} is inverted, just as the direction of motion of a screw changes when its rotation is reversed. This fact could, for example, in principle, allow one to distinguish between left- and right-handed chiral carbon nanotubes [5].

A second observation, made only recently [6–8], is that the magnitude of α is proportional to the strength of electron-electron (e - e) interactions in the sample, and it can, thus, in principle, be used to deduce the interaction strength. This is true at both high and low temperature T . In the high- T limit, α can be calculated using a Boltzmann equation approach [6], and it is found to be proportional to the e - e scattering rate or to β^2 , where β is the interaction parameter. In the low- T (mesoscopic) limit, it can be calculated either by general diagrammatic techniques [7,9] or within the Landauer picture of single-particle scattering from a self-consistent potential [8,10], and it is then found that $\alpha \propto \beta$. The Landauer picture affords a

simple understanding of this result, as follows. The Onsager symmetry is obeyed at each energy. In the absence of interactions, the total current is the sum over contributions at all energies and is, thus, also even in B , and so α is zero. However, the electric field due to the applied voltage V induces changes in the local current and electron densities which contain B -odd components (as happens, for example, in the Hall effect). If there are interactions, these density changes produce B -odd components in the scattering potential, and, therefore, in χ , which are proportional to β .

It is well known that e - e interactions are important in single-walled carbon nanotubes because of their one-dimensional (1D) electronic dispersion [11]. Describing the conduction electrons in an infinite clean nanotube as a Luttinger liquid [12,13] allows one to explain the power-law energy dependences of tunneling rates seen in several transport experiments [14,15]. However, real nanotubes are finite in length and often disordered, and the nature of transport in them at high and low T remains an open question. For this reason, we chose them as a test system in which to carry out the first specific and detailed measurements of nonlinear coefficients χ and α . We exploit the fact that, in a nanotube, unlike a pure 1D system, there is a simple mechanism for generating magnetotransport effects: The dispersion is modified by a magnetic field along the tube axis due to the Aharonov-Bohm phase [6,16]. Our results are in agreement with the general expectations of the theory. Near room temperature, α is small and its sign is independent of gate voltage, whereas as T is decreased, α develops random mesoscopic fluctuations. In addition, we find magnetoresistance in nanotubes in the metallic regime persisting up to room temperature. Our results suggest that basic theoretical questions about magnetotransport in a 1D electron system remain to be addressed.

Each device consists of an individual single-walled carbon nanotube formed by chemical vapor growth from iron catalyst particles [17,18], with two gold contacts patterned by thermal evaporation through a stencil. The substrate is 450 nm of thermal SiO_2 on a highly n -doped silicon wafer,

to which a gate voltage V_g is applied through a 10 M Ω resistor. An atomic force microscope image of a device (device 1) containing a nanotube of diameter $d \sim 1.3$ nm and length $L = 4$ μm between the contacts is shown in Fig. 1(a), along with the arrangement used to measure G and χ . A sinusoidal bias of rms amplitude V_0 at frequency f (650 Hz) is applied to one contact, with the other connected to a virtual-earth current preamplifier (Ithaco 1211). A 10 μF capacitor in series enforces zero dc current. The rms harmonic current components I_f and I_{2f} are extracted using lock-in amplifiers. In all the measurements, V_0 is kept sufficiently small ($\sim kT/e$) to ensure that $I_{2f} \ll I_f$ and that $I_{2f} \propto V_0^2$, so that harmonics beyond I_{2f} are negligible. The first two coefficients in Eq. (1) can then be obtained as $G = I_f/V_0$ and $\chi = 2I_{2f}/V_0^2$. We found α to be nonzero in all three devices studied. We made detailed measurements on one metallic nanotube (device 1) and one semiconducting nanotube (device 2). We focus here on the metallic device for brevity and because band-gap effects complicate the interpretation of nonlinear behavior in semiconducting devices.

Before considering the nonlinear measurements, it is necessary to analyze the linear transport properties. The linear behavior of device 1 at $B = 0$ is illustrated in

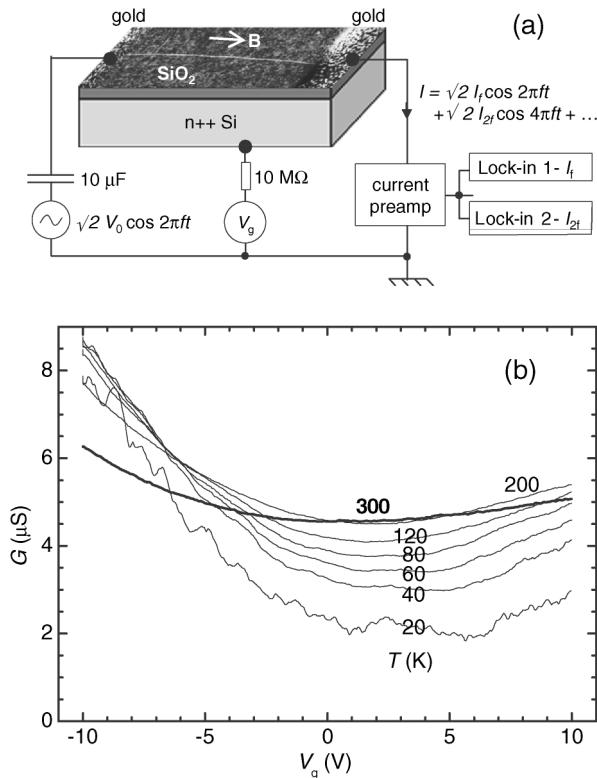


FIG. 1. (a) Tapping-mode atomic force microscope image of device 1 combined with a schematic diagram of the measurement setup. The separation of the gold contacts is 4 μm . The orientation of the magnetic field parallel to the nanotube is indicated. (b) Linear conductance vs gate voltage at a series of temperatures.

Fig. 1(b). The weak dependence on V_g at room temperature is characteristic of a metallic nanotube. We have also made detailed measurements on a semiconducting nanotube (device 2), although the strong V and T dependences arising from band-gap effects make interpreting the nonlinear behavior more difficult. In device 1, as T is decreased from 300 K, G rises and passes through a maximum at a temperature which depends on V_g before falling again. For $T < 20$ K, a dense “grass” of aperiodic and unreproducible Coulomb blockade oscillations appears (not shown), and, by $T = 4.2$ K, G is too small to measure.

The negative value of dG/dT at room temperature indicates that the resistance is not dominated by the contacts, since poor contacts would ensure positive dG/dT [14]. We also know from characterizing many similar devices that our contacts are reliable and have high transparency; i.e., the contact resistance R_c is not much larger than the ideal value of $h/4e^2$. If we assume the additional resistance is distributed along the nanotube, then in the high- T limit it can be characterized by a backscattering length l_b given by $G^{-1} = R_c + (h/4e^2)L/l_b$ [19,20]. At 300 K, $G \sim 5$ μS , and we find $l_b > \sim 150$ nm. This is shorter than the phonon scattering length, which is about 1.6 μm [20], implying that backscattering is predominantly due to disorder, although some phonon scattering is needed to explain the negative dG/dT at room T . This is consistent with the behavior in the low T regime, where, from the Coulomb blockade, we infer that the nanotube breaks up electrically into a series of submicron islands [21]. We do not know the precise origin of the disorder, which is much higher than in the cleanest nanotube devices [20]. It may be explained by contaminants associated with our growth process.

The effects of magnetic field on the linear conductance are illustrated in Fig. 2. At room T , G decreases approximately quadratically with B up to ± 16 T. Fitting it to $G(B) = (1 + \gamma B^2)G_0$ at each gate voltage, we find that the parameter γ varies steadily from about -2×10^{-4} T^{-2} at $V_g = 0$ to -4×10^{-4} T^{-2} at $V_g = 5$ V. In the semiconducting device at 200 K, we found γ to be *positive*, reaching a peak of $+4 \times 10^{-3}$ T^{-2} close to threshold but maintaining a value of $+2 \times 10^{-4}$ T^{-2} in the metallic regime. A positive magnetoconductance near threshold in a semiconducting nanotube can be explained by a decreasing band gap [6,16,22,23]. (The contribution of the gold leads to the resistance is negligible.) However, to our knowledge, no mechanism has been put forward to explain significant magnetoconductance in the metallic regime.

As T decreases, G develops nonperiodic oscillations as a function both of V_g [see Fig. 1(b)] and of B [see Fig. 2(a)]. Figure 2(b) is a gray-scale plot of $G(V_g, B)$ at 20 K. Figure 2(c) is a histogram of the B -symmetrized and anti-symmetrized parts of G at 20 K, showing that the antisymmetric part is much smaller than the symmetric part. Since the absence of an antisymmetric component is required by Onsager symmetry, this is evidence that our measurement is indeed effectively two-terminal. [The visible deviation

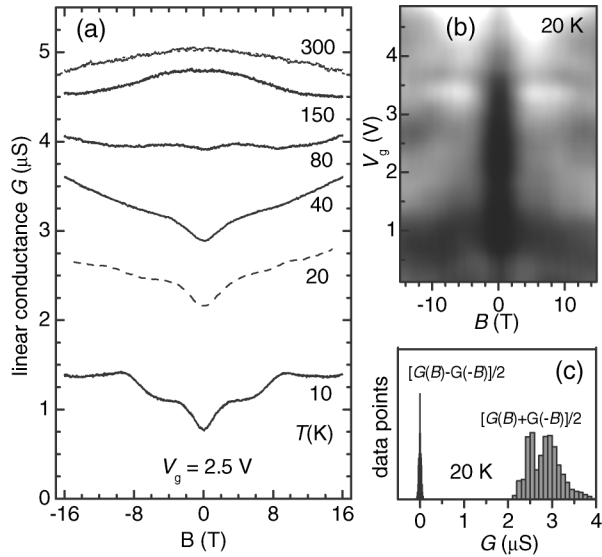


FIG. 2. (a) Linear conductance G vs magnetic field B at a series of temperatures for a fixed gate voltage, measured using the setup in Fig. 1(b). (b) Gray-scale plot of $G(V_g, B)$ at $T = 20$ K. Black is $2.2 \mu\text{S}$, white is $3.5 \mu\text{S}$. (c) Histogram of B -symmetrized and B -antisymmetrized parts of G , averaged over all V_g and B , from the data set in (b).

from symmetry about $B = 0$ in the 20 K (dashed line) sweep in Fig. 2(a), and the broadening of the black peak in Fig. 2(c), resulted from drift over the two-hour time scale of the magnetic-field sweep.]

Oscillations as a function of V_g and B are predicted by a single-particle model of quantum interference [23,24] in the presence of multiple scatterers. In this model, one anticipates a characteristic magnetic-field period $B_c \sim 4(h/e)/(L_{\text{eff}}d)$, corresponding to the change in magnetic flux which alters the phase difference between typical electron paths in the K and K' subbands by 2π . Estimating the effective path length L_{eff} to be the lesser of the nanotube length L and the thermal length $L_T \sim hv_F/k_B T$, where $v_F = 8 \times 10^5 \text{ ms}^{-1}$ is the Fermi velocity, for $T = 20$ K we obtain $L_{\text{eff}} \sim L_T \sim 2 \mu\text{m}$ and $B_c \sim 6$ T. This is compatible with the oscillations seen in Fig. 2(a). The model also predicts a gate voltage oscillation period $\sim hv_F/(eL_{\text{eff}})$ of a few mV (taking into account that the capacitance is dominated by the gate). Such short-period oscillations would not be resolved in these measurements. However, it is clear that there are features in Fig. 2(b) which vary much more slowly with V_g . In particular, at 20 K there is a dip at $B = 0$ with a half-width of ~ 2 T persisting over the entire range of V_g . A similar feature was observed in device 2 in its metallic state at negative gate voltage. Analogous behavior was very recently reported for single-walled nanotubes in a perpendicular field [25]. In 2D and 3D metals and multiwalled nanotubes [26], such a dip is expected due to weak localization, but the corresponding effect in a 1D system with B -dependent dispersion appears not to have been considered before.

We now turn to the measurements of the nonlinear coefficient χ . Figures 3(a)–3(c) are gray-scale plots of $\chi(V_g, B)$ at three different temperatures. Figures 3(d) and 3(e) show line traces of χ vs B at two selected gate voltages. At the highest temperature (200 K, bold traces), χ is small and varies slowly with B up to ± 16 T. Like G , χ develops oscillations as a function of both V_g and B as the sample is cooled. In contrast with G , however, χ is not symmetric about $B = 0$. Figures 3(f) and 3(g) are gray-scale plots of the symmetric and antisymmetric parts of χ at $T = 20$ K. Very similar behavior was seen in device 2 in the metallic regime.

Note that χ depends on both the intrinsic asymmetry of the device and the asymmetry of the measurement [Fig. 1(a)]: Applying a bias V_0 to the source generates a nonlinear “self-gating” current $I_{2f,sg} \sim (dG/dV_g)V_0^2/4$ due to the change in G caused by the resulting change in the average potential difference between gate and nanotube [27]. This current contribution must, like G , be symmetric in B and cannot contribute to the B -antisymmetric part of χ reported above.

To date, there exist no predictions specific to nanotubes with which we can quantitatively compare these measurements of χ . Nevertheless, the theory mentioned in the

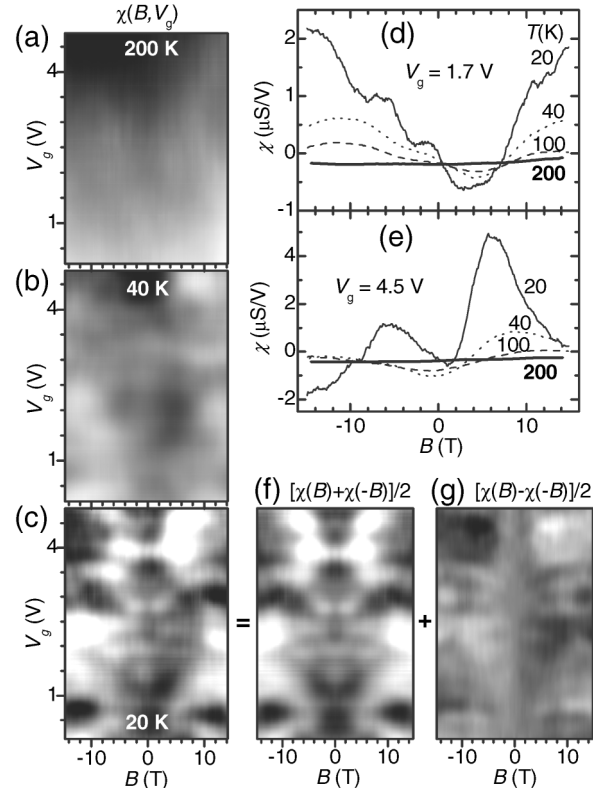


FIG. 3. (a) Variation of the nonlinear coefficient χ with magnetic field and temperature. (a)–(c) Gray-scale plots of $\chi(B, V_g)$ at $T = 200, 40,$ and 20 K, respectively. (d),(e) Traces of χ vs B at a series of temperatures for $V_g = 1.7$ V and $V_g = 4.5$ V, respectively. (f),(g) Gray-scale plots of the B -symmetric and B -antisymmetric parts, respectively, of χ at $T = 20$ K.

introduction leads to qualitative expectations for the behavior of the B -linear coefficient α in Eq. (2). At high T , the sign of α should depend on the handedness of the nanotube [5,6]. In this regime, α should vary slowly, without oscillating, as a function of Fermi energy and, thus, of V_g . At low T , in the mesoscopic regime, as a result of disorder, one expects mesoscopic fluctuations of α characterized by correlation functions [7]. Since the disorder should have no preferred chirality, one expects $\langle \alpha \rangle = 0$, where the average is taken over disorder realizations. In addition, Ref. [7] predicts $\langle \alpha^2 \rangle \propto \beta^2/T^2$ for a normal mesoscopic metallic sample.

We extracted values of α from the data by fitting a straight line of the form $\chi_0 + \alpha B$ to the data points of χ vs B in the range $-2 \text{ T} < B < +2 \text{ T}$, doing so at each value of V_g and T . The results for α are shown in Fig. 4. At the highest temperature (200 K), α is small and varies slowly with V_g without changing sign. This is consistent with the above expectations. As T decreases, α develops oscillations which cause its sign to alternate as a function of V_g , again consistent with the expectations. In the inset, we plot $\langle \alpha^2 \rangle$, obtained by averaging α^2 over V_g , against T . The results are consistent with the $1/T^2$ dependence (solid line) mentioned above, in spite of the ostensible inapplicability of the calculation in Ref. [7].

In summary, we have carried out the first experimental study of a new transport coefficient in nanoscale devices, namely, the magnitude of the V^2B term in the I - V characteristics. This coefficient provides a way to quantify the electron-electron interaction strength, which is of particular interest in our chosen system of single-walled carbon nanotubes. We also find unexplained magnetoresistance in disordered metallic nanotubes at high and low temperatures that acts as a further indication that basic aspects of these 1D conductors remain to be addressed.

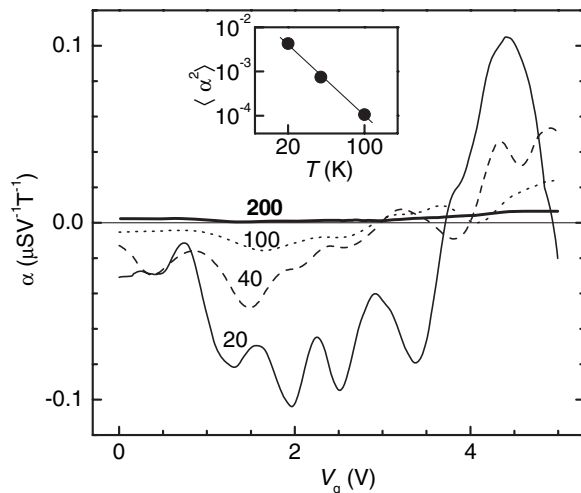


FIG. 4. (a) Variation of the V^2B coefficient α with V_g at a series of temperatures. Inset: log-log plot of $\langle \alpha^2 \rangle$ vs T , where the straight line indicates a $1/T^2$ dependence.

We thank A. Andreev, E. Deyo, B. Spivak, O. Vilches, and N. Wilson for many useful discussions and J. Chen for providing the catalyst particles. This work was supported in part by the UW Royalty Research Fund and by an NSF IGERT program.

*Corresponding author.

Electronic address: cobden@u.washington.edu

- [1] L. Onsager, Phys. Rev. **38**, 2265 (1931).
- [2] L. Landau and E.M. Lifshitz, *Statistical Physics* (Butterworth-Heinemann, Washington, DC, 1980), Vol 1.
- [3] B.I. Sturman and V.M. Fridkin, *The Photovoltaic and Photorefractive Effects in Non-Centrosymmetric Materials* (Gordon and Breach, New York, 1992).
- [4] G.L.J.A. Rikken, J. Folling, and P. Wyder, Phys. Rev. Lett. **87**, 236602 (2001).
- [5] V. Krstic *et al.*, J. Chem. Phys. **117**, 11 315 (2002).
- [6] E.L. Ivchenko and B. Spivak, Phys. Rev. B **66**, 155404 (2002).
- [7] B. Spivak and A. Zyuzin, Phys. Rev. Lett. **93**, 226801 (2004).
- [8] D. Sanchez and M. Buttiker, Phys. Rev. Lett. **93**, 106802 (2004).
- [9] A. Larkin and D. Khmel'nitskii, Sov. Phys. JETP **91**, 1815 (1986); V. Fal'ko and D. Khmel'nitskii, Sov. Phys. JETP **68**, 186 (1989).
- [10] M. Buttiker, IBM J. Res. Dev. **32**, 317 (1988).
- [11] D. Mattis, *The Many-Body Problem: An Encyclopedia of Exactly Solved Models in One Dimension* (World Scientific, Singapore, 1992).
- [12] C. Kane, L. Balents, and M.P.A. Fisher, Phys. Rev. Lett. **79**, 5086 (1997).
- [13] A. Komnik, R. Egger, and A.O. Gogolin, Phys. Rev. B **56**, 1153 (1997).
- [14] M. Bockrath *et al.*, Nature (London) **397**, 598 (1999).
- [15] Z. Yao, H.W.C. Postma, L. Balents, and C. Dekker, Nature (London) **402**, 273 (1999).
- [16] H. Ajiki and T. Ando, Physica (Amsterdam) **201B**, 349 (1994).
- [17] J. Kong, A.M. Cassell, and H. Dai, Chem. Phys. Lett. **292**, 567 (1998).
- [18] Y. Li, J. Liu, Y.Q. Wang, and Z.L. Wang, Chem. Mater. **13**, 1008 (2001).
- [19] S. Datta, *Electronic Transport in Mesoscopic Systems* (Cambridge University Press, Cambridge, England, 1995).
- [20] J. Y. Park *et al.*, Nano Lett. **4**, 517 (2004).
- [21] P.L. McEuen *et al.*, Phys. Rev. Lett. **83**, 5098 (1999).
- [22] E.D. Minot *et al.*, Nature (London) **428**, 536 (2004).
- [23] J. Cao *et al.*, Phys. Rev. Lett. **93**, 216803 (2004).
- [24] W. Liang *et al.*, Nature (London) **411**, 665 (2001).
- [25] H.T. Man and A.F. Morpurgo, Phys. Rev. Lett. **95**, 026801 (2005).
- [26] L. Langer *et al.*, Phys. Rev. Lett. **76**, 479 (1996); A. Bachtold *et al.*, Nature (London) **397**, 673 (1999); B. Stojetz *et al.*, Phys. Rev. Lett. **94**, 186802 (2005).
- [27] A. Lofgren *et al.*, Phys. Rev. Lett. **92**, 046803 (2004).